

Unified Approach to the Large-Signal and High-Frequency Theory of $p-n$ -Junctions

Anatoly A. Barybin*, and Edval J. P. Santos**

**Electronics Department,
Saint-Petersburg State Electrotechnical University,
197376, Saint-Petersburg, Russia*

***Laboratory for Devices and Nanostructures,
Departamento de Eletrônica e Sistemas,
Universidade Federal de Pernambuco,
C.P. 7800, 50670-000, Recife-PE, Brasil
E-mail: edval@ee.ufpe.br*

Spectral approach to the charge carrier transport in $p-n$ -junctions has allowed us to revise the theoretical results relating to large signal operation of the junction to make them valid for both the low and high frequencies ranges. The spectral composition of the external circuit current includes both the DC and AC components. The former produces the static current–voltage characteristic with the modified Bessel function of zeroth order, $I_0(\beta V_{\sim})$, while the latter yields the dynamic admittance with the modified Bessel function of first order, $I_1(\beta V_{\sim})$, either of them depend on the signal amplitude. Our experimental results are consistent with the theoretical ones if a fitting parameter allowing for recombination processes in the depletion layer is taken into account.

Keywords:

I. INTRODUCTION

The conventional theory of $p-n$ -junctions is usually studied in two limiting cases: small-signal/high-frequency and large-signal/low-frequency [1, 2, 3, 4, 5, 6]. We have found out that it is possible to unify these two cases by applying the spectral analysis to calculating the external circuit current for a $p-n$ -diode. General scheme of finding the spectral solution to the diffusion equations for the $p-n$ -junction under arbitrary signal action is developed in Sec. II and then applied in Sec. III to calculate the external circuit current. For this work, it is assumed that the relaxation times, and the diffusion constants do not change with injection level, or constant effective values are used. The nonlinearity considered in this work is related to the doping profile, as it yields a semiconducting $p-n$ -junction. Sections IV and V deal with the static current–voltage and dynamic characteristics of the diode. First measurements to validate the experimental setup is set forth in Sec. VI. Appendix examines the conventional approach (based on applying the customary current–voltage characteristic expression to time-varying conditions) to be compared with our results obtained below in terms of the spectral approach.

II. SPECTRAL SOLUTION OF DIFFUSION EQUATIONS

Theoretical basis of the charge carrier transport in $p-n$ -junctions is the diffusion–drift equations for minority carriers in the n - and p -regions. These equations are derived from the continuity equations together with the current density expressions for holes and electrons. Such diffusion–drift equations have the following one-dimensional form [4, 5]:

(a) for holes (with equilibrium and nonequilibrium densities p_n and $p(z, t)$) injected into the n -region

$$\frac{\partial p}{\partial t} + \frac{\partial(p\mu_p E)}{\partial z} - \frac{\partial^2(D_p p)}{\partial z^2} + \frac{p - p_n}{\tau_p} = 0, \quad (1)$$

(b) for electrons (with equilibrium and nonequilibrium densities n_p and $n(z, t)$) injected into the p -region

$$\frac{\partial n}{\partial t} - \frac{\partial(n\mu_n E)}{\partial z} - \frac{\partial^2(D_n n)}{\partial z^2} + \frac{n - n_p}{\tau_n} = 0. \quad (2)$$

We shall apply Eqs. (1) and (2) to study the simplest Shockley's model of the ideal diode [1] but operating at the nonlinear and multifrequency regime under action of the harmonic signal of arbitrary amplitude. In the case of low-level injection in $p-n$ -diodes, one conventionally assumes $E = 0$ for the neutral parts of the p - and n -regions [4, 5]. Then Eqs. (1) and (2) turn into the diffusion equations for the excess concentrations (over their equilibrium values p_n and n_p) for holes, $\Delta p(z, t) = p(z, t) - p_n$, and for electrons, $\Delta n(z, t) = n(z, t) - n_p$, of the following form:

$$\left(1 + \tau_p \frac{\partial}{\partial t}\right) \Delta p - L_p^2 \frac{\partial^2 \Delta p}{\partial z^2} = 0, \quad (3)$$

$$\left(1 + \tau_n \frac{\partial}{\partial t}\right) \Delta n - L_n^2 \frac{\partial^2 \Delta n}{\partial z^2} = 0, \quad (4)$$

where $L_p = \sqrt{D_p \tau_p}$ and $L_n = \sqrt{D_n \tau_n}$ are the diffusion lengths for holes and electrons, respectively.

For the resonant circuit connection, the total voltage applied to the $p-n$ -diode consists of the DC bias voltage V_0 and the harmonic signal voltage $V_{\sim} \cos \omega t$:

$$v(t) = V_0 + V_{\sim} \cos \omega t. \quad (5)$$

Nonlinearity of electronic processes in the $p-n$ -junction produces frequency harmonics $k\omega$ so that the required solutions of Eqs. (3) and (4) can be represented in the complex form of Fourier series:

$$\Delta p(z, t) = \sum_{k=-\infty}^{\infty} \Delta p_k(z) e^{ik\omega t}, \quad (6)$$

$$\Delta n(z, t) = \sum_{k=-\infty}^{\infty} \Delta n_k(z) e^{ik\omega t}. \quad (7)$$

Real values of $\Delta p(z, t)$ and $\Delta n(z, t)$ are provided with the following relations for the complex amplitudes: $\Delta p_k = \Delta p_{-k}^*$ and $\Delta n_k = \Delta n_{-k}^*$.

Substitution of the required solutions (6) and (7) into Eqs. (3) and (4) with taking into account the orthogonality of harmonics reduces to the following equations for the desired complex amplitudes of harmonics:

$$\frac{d^2 \Delta p_k}{dz^2} - \frac{\Delta p_k}{L_{pk}^2} = 0 \quad \text{and} \quad \frac{d^2 \Delta n_k}{dz^2} - \frac{\Delta n_k}{L_{nk}^2} = 0 \quad (8)$$

with

$$L_{pk} = \frac{L_p}{\sqrt{1 + ik\omega\tau_p}} \quad \text{and} \quad L_{nk} = \frac{L_n}{\sqrt{1 + ik\omega\tau_n}}.$$

General solutions of equations (8) for the $p-n$ -diode with the junction region $-W_p < z < W_n$ have the following form:

(a) for holes injected into the n -region ($z \geq W_n$)

$$\Delta p_k(z) = C_{pk}^+ \exp\left(-\Lambda_{pk} \frac{z - W_n}{L_p}\right) + C_{pk}^- \exp\left(\Lambda_{pk} \frac{z - W_n}{L_p}\right), \quad (9)$$

where $\Lambda_{pk} = a_{pk} + ib_{pk}$ and

$$a_{pk} = \frac{1}{\sqrt{2}} \sqrt{1 + \sqrt{1 + (k\omega\tau_p)^2}}, \quad b_{pk} = \frac{k\omega\tau_p}{2a_{pk}}; \quad (10)$$

(b) for electrons injected into the p -region ($z \leq -W_p$)

$$\Delta n_k(z) = C_{nk}^+ \exp\left(-\Lambda_{nk} \frac{z + W_p}{L_n}\right) + C_{nk}^- \exp\left(\Lambda_{nk} \frac{z + W_p}{L_n}\right), \quad (11)$$

where $\Lambda_{nk} = a_{nk} + ib_{nk}$ and

$$a_{nk} = \frac{1}{\sqrt{2}} \sqrt{1 + \sqrt{1 + (k\omega\tau_n)^2}}, \quad b_{nk} = \frac{k\omega\tau_n}{2a_{nk}}. \quad (12)$$

According to Eqs. (10) and (12), always $\text{Re}\Lambda_{pk} = a_{pk} > 0$ and $\text{Re}\Lambda_{nk} = a_{nk} > 0$. So for the $p-n$ -diodes with thick base (when $d_n \gg L_p$ and $d_p \gg L_n$, where d_n and d_p are thicknesses of the neutral parts) we can take $C_{pk}^- = 0$ and $C_{nk}^+ = 0$. This eliminates the necessity for boundary conditions on ohmic contacts. Taking into account (9) and (11) with $C_{pk}^- = C_{nk}^+ = 0$, the general solutions (6) and (7) of Eqs. (3) and (4) assume the form

$$\Delta p(z, t) = \sum_{k=-\infty}^{\infty} C_{pk}^+ \exp\left(-\Lambda_{pk} \frac{z - W_n}{L_p}\right) e^{ik\omega t}, \quad (13)$$

$$\Delta n(z, t) = \sum_{k=-\infty}^{\infty} C_{nk}^- \exp\left(\Lambda_{nk} \frac{z + W_p}{L_n}\right) e^{ik\omega t}. \quad (14)$$

These expressions provide for $\Delta p(z, t) \rightarrow 0$ as $z \rightarrow \infty$ and $\Delta n(z, t) \rightarrow 0$ as $z \rightarrow -\infty$ because of $\text{Re}\Lambda_{pk} > 0$ and $\text{Re}\Lambda_{nk} > 0$.

The constants C_{pk}^+ and C_{nk}^- in Eqs. (13) and (14) can be found from the conventional injection boundary conditions [4, 5]:

$$\Delta p(W_n, t) = p_n f(t) \quad \text{for } z = W_n, \quad (15)$$

$$\Delta n(-W_p, t) = n_p f(t) \quad \text{for } z = -W_p, \quad (16)$$

where for the applied voltage $v(t)$ of the form (5) we have introduced the function

$$f(t) = \exp\left(\frac{qv(t)}{\kappa T}\right) - 1. \quad (17)$$

where $\kappa = 1.38 \times 10^{-23} J/K$ is the Boltzmann constant, and T is the temperature in kelvin.

Substitution of (13) and (14) into the boundary conditions (15) and (16) yields

$$\sum_{k=-\infty}^{\infty} C_{pk}^+ e^{ik\omega t} = p_n f(t), \quad (18)$$

$$\sum_{k=-\infty}^{\infty} C_{nk}^- e^{ik\omega t} = n_p f(t). \quad (19)$$

By using the orthogonality property of harmonics in the expansions (18) and (19), it is easy to obtain the desired constants:

$$C_{pk}^+ = p_n F_k \quad \text{and} \quad C_{nk}^- = n_p F_k, \quad (20)$$

where F_k is the Fourier amplitude of the k th harmonic for the function $f(t)$ given by Eq. (17), that is

$$F_k = \frac{1}{2\pi} \int_{-\pi}^{\pi} f(t) e^{-ik\omega t} d\omega t. \quad (21)$$

Substitution of the function (17) into formula (21) gives

$$F_0 = I_0(\beta V_{\sim}) \exp(\beta V_0) - 1 \quad \text{for } k = 0, \quad (22)$$

$$F_k = F_{-k} = I_k(\beta V_{\sim}) \exp(\beta V_0) \quad \text{for } k \neq 0. \quad (23)$$

Here we have introduced the modified Bessel functions of the first kind of order k ($k = 0, \pm 1, \pm 2, \dots$) which have the following integral representation (see, for example, formula 8.431.5 in [7]):

$$I_k(\beta V_{\sim}) = \frac{1}{\pi} \int_0^{\pi} e^{\beta V_{\sim} \cos \omega t} \cos k\omega t d\omega t. \quad (24)$$

These functions depend on βV_{\sim} , where V_{\sim} is an amplitude of the signal applied to the p - n -junction and $\beta = q/\kappa T$.

Consequently, with making allowance for (20) the general solutions (13) and (14) of the diffusion equations (3) and (4) take the final form of spectral expansions:

$$\Delta p(z, t) = p_n \sum_{k=-\infty}^{\infty} F_k \exp\left(-\Lambda_{pk} \frac{z - W_n}{L_p}\right) e^{ik\omega t}, \quad (25)$$

$$\Delta n(z, t) = n_p \sum_{k=-\infty}^{\infty} F_k \exp\left(\Lambda_{nk} \frac{z + W_p}{L_n}\right) e^{ik\omega t}. \quad (26)$$

These expressions allow us to obtain the spectral composition of the current flowing through an external circuit connected to the $p-n$ -diode.

III. EXTERNAL CIRCUIT CURRENT FOR $p-n$ -DIODES

The initial equation to derive an expression for the diode current is the total current conservation law of the general form $\nabla \cdot (\mathbf{j}_p + \mathbf{j}_n + \epsilon \partial \mathbf{E} / \partial t) = 0$ following from Maxwell's equations. Its one-dimensional form (along the z -direction) is

$$\frac{\partial}{\partial z} \left(j_{pz} + j_{nz} + \epsilon \frac{\partial E_z}{\partial t} \right) = 0. \quad (27)$$

The quantity in parentheses of Eq. (27), being independent of z , defines the external circuit current (for the cross-section area S of the diode) as a function of time:

$$\begin{aligned} J(t) &\equiv j_{pz}(z, t)S + j_{nz}(z, t)S + \epsilon \frac{\partial E_z(z, t)}{\partial t} S \\ &= q(\mu_p p + \mu_n n) E_z S - q \left(D_p \frac{\partial p}{\partial z} - D_n \frac{\partial n}{\partial z} \right) S + \epsilon \frac{\partial E_z}{\partial t} S. \end{aligned} \quad (28)$$

We have used the usual expressions for the hole and electron current densities [5] involving the drift and diffusion components which underlie the initial diffusion–drift equations (1) and (2). All the terms on the right of Eq. (28) depend on both z and t , but taken together in any cross section they yield the external circuit current as a function of only time.

Restricting our consideration to the $p-n$ -diodes with low injection ($p \ll n_n$ but $p > p_n$ so that the excess hole density is $\Delta p = p - p_n > 0$, for n -type, similar conditions hold for p -type), as was noted above, we can assume $E_z = 0$ in neutral parts of the p - and n -regions [5]. Then the external circuit current (28) is determined only by the diffusion currents taken at any cross section, for example, at $z = W_n$:

$$\begin{aligned} J(t) &= -qD_p \frac{\partial p(z, t)}{\partial z} \Big|_{z=W_n} S + qD_n \frac{\partial n(z, t)}{\partial z} \Big|_{z=W_n} S \\ &\equiv j_{pz}(W_n, t)S + j_{nz}(W_n, t)S. \end{aligned} \quad (29)$$

Neglecting recombination processes inside the $p-n$ -junction (which is true if $W_n \ll L_p$ and $W_p \ll L_n$) we can write [5]

$$j_{nz}(W_n, t) = j_{nz}(-W_p, t). \quad (30)$$

Substitution of (30) into Eq. (29) gives the external circuit current:

$$\begin{aligned} J(t) &= j_{pz}(W_n, t)S + j_{nz}(-W_p, t)S \\ &= -qD_p \frac{\partial \Delta p(z, t)}{\partial z} \Big|_{z=W_n} S + qD_n \frac{\partial \Delta n(z, t)}{\partial z} \Big|_{z=-W_p} S, \end{aligned} \quad (31)$$

where $\Delta p = p - p_n$ and $\Delta n = n - n_p$ are the excess concentrations of injected carriers given by Eqs. (25) and (26). Inserting these formulas into expression (31), we finally obtain the spectral representation for the external circuit current:

$$J(t) = J_{s,p} \sum_{k=-\infty}^{\infty} F_k \Lambda_{pk} e^{ik\omega t} + J_{s,n} \sum_{k=-\infty}^{\infty} F_k \Lambda_{nk} e^{ik\omega t}. \quad (32)$$

Here, the hole and electron contributions into the saturation current of the thick p - n -diode are defined, as it is generally accepted [4, 5], in the following form:

$$J_{s,p} = \frac{qp_n D_p}{L_p} S \quad \text{and} \quad J_{s,n} = \frac{qn_p D_n}{L_n} S. \quad (33)$$

Expression (32) contains all the spectral components of the external circuit current, among which the terms with numbers $k = 0$ (the DC current) and $k = \pm 1$ (the AC current) are of most interest for our subsequent consideration.

IV. STATIC CURRENT-VOLTAGE CHARACTERISTIC OF p - n -DIODES

The term in series (32) numbered by $k = 0$ corresponds to the DC current J_0 , which by using expression (22) for F_0 and $\Lambda_{p0} = \Lambda_{n0} = 1$ can be written in the form of the *static current-voltage characteristic*:

$$J_0(V_0, V_{\sim}) = J_s \left[I_0(\beta V_{\sim}) e^{\beta V_0} - 1 \right]. \quad (34)$$

Here, $I_0(\beta V_{\sim})$ is the modified Bessel function of zeroth order depending on the signal amplitude V_{\sim} . The saturation current J_s has the customary form [4, 5]

$$J_s = J_{s,p} + J_{s,n} = \frac{qp_n D_p}{L_p} S + \frac{qn_p D_n}{L_n} S. \quad (35)$$

Expression (34) differs in appearing the Bessel function $I_0(\beta V_{\sim})$ from the customary current-voltage characteristic given in such well-known books as, for example, [4, 5]. Coincidence between them takes place only when $I_0(\beta V_{\sim}) \simeq 1$, which is true for small signals with $V_{\sim} \ll \kappa T/q$. However, an expression similar to our equation (34) was found in a less-known textbook [6] [8] written in German, whose derivation is adduced for comparison in Appendix (see formula (A4)).

The modified Bessel function $I_0(\beta V_{\sim}) \geq 1$ as a function of the signal amplitude V_{\sim} mathematically reflects the so-called effect of *signal rectification*. This effect provides a contribution into the DC current J_0 from the signal and results in up-shifts of the static current-voltage characteristic $J_0(V_0)$ with increasing V_{\sim} , as shown in Fig. 1.

V. DYNAMIC CHARACTERISTICS OF p - n -DIODES

The first harmonic current contribution to the general expression (32) for the external current corresponds to terms numbered by $k = \pm 1$ and is equal to

$$J_1(t) = J_1 e^{i\omega t} + c.c. \quad \text{with} \quad J_1 = F_1 (J_{s,p} \Lambda_{p1} + J_{s,n} \Lambda_{n1}), \quad (36)$$

where the quantities Λ_{p1} , Λ_{n1} , F_1 are respectively given by Eqs. (10), (12), (23) for $k = 1$.

Expressions (5) with $V_{\sim} = 2V_1$ and (36) allow one to introduce for the p - n -diode its *dynamic admittance* defined as

$$Y = \frac{J_1}{V_1} \equiv G_d + i\omega C_d. \quad (37)$$

Here, the *dynamic conductance* G_d and the *dynamic (diffusion) capacitance* C_d are introduced in a customary way [5]. After substituting (36) into (37) and some transformations we obtain these quantities as functions of frequency:

$$G_d(\omega) = gG_0 \left(a_{p1}(\omega) \frac{J_{s,p}}{J_s} + a_{n1}(\omega) \frac{J_{s,n}}{J_s} \right), \quad (38)$$

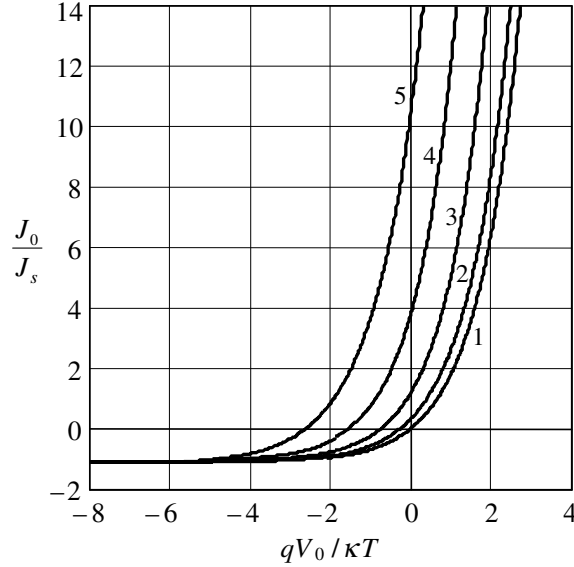


FIG. 1: Static current–voltage characteristics for different values of the signal voltage amplitudes: $V_{\sim} = 0$ (curve 1), $\kappa T/q$ (curve 2), $2\kappa T/q$ (curve 3), $3\kappa T/q$ (curve 4), $4\kappa T/q$ (curve 5).

$$C_d(\omega) = \frac{gG_0}{\omega} \left(b_{p1}(\omega) \frac{J_{s,p}}{J_s} + b_{n1}(\omega) \frac{J_{s,n}}{J_s} \right), \quad (39)$$

where the quantities a_{p1}, b_{p1} and a_{n1}, b_{n1} follow from Eqs. (10) and (12) with $k = 1$.

Formulas (38) and (39) have been derived by inserting the differential conductance introduced from the static current–voltage characteristic $J_0(V_0, V_{\sim})$ defined as

$$G_0 = \frac{\partial J_0(V_0, V_{\sim})}{\partial V_0}. \quad (40)$$

The static current–voltage characteristic, Eq. (34), gives the differential conductance (40) which depends on both the bias voltage V_0 and the signal amplitude V_{\sim} :

$$G_0(V_0, V_{\sim}) = \frac{J_0 + J_s}{\kappa T/q} = \frac{J_s \exp(\beta V_0)}{\kappa T/q} I_0(\beta V_{\sim}). \quad (41)$$

Formulas (38) and (39) contain a combination of the modified Bessel functions $I_0(\beta V_{\sim})$ and $I_1(\beta V_{\sim})$ in the form of a factor:

$$g(V_{\sim}) = \frac{2}{\beta V_{\sim}} \frac{I_1(\beta V_{\sim})}{I_0(\beta V_{\sim})} \equiv \frac{g_1(V_{\sim})}{I_0(\beta V_{\sim})} \leq 1 \quad (42)$$

with

$$g_1(V_{\sim}) = \frac{I_1(\beta V_{\sim})}{\beta V_{\sim}/2}. \quad (43)$$

These quantities depend on the signal amplitude V_{\sim} , so that $g(V_{\sim}) \simeq g_1(V_{\sim}) \simeq 1$ for small signals when $V_{\sim} \ll \kappa T/q$ and $g(V_{\sim}) \simeq 2/(\beta V_{\sim}) \rightarrow 0$ as $V_{\sim} \rightarrow \infty$, whereas here $g_1(V_{\sim})$ is approximated by an exponentially growing function.

After inserting (41) and (42) into Eqs. (38) and (39), they take the following form:

$$G_d(\omega) = g_1 G_{d0} \left(a_{p1}(\omega) \frac{J_{s,p}}{J_s} + a_{n1}(\omega) \frac{J_{s,n}}{J_s} \right), \quad (44)$$

$$C_d(\omega) = g_1 C_{d0} \left(a_{p1}^{-1}(\omega) \frac{Q_p}{Q} + a_{n1}^{-1}(\omega) \frac{Q_n}{Q} \right), \quad (45)$$

where $Q = Q_p + Q_n$ with $Q_p \equiv J_{s,p}\tau_p = qp_nL_pS$ and $Q_n \equiv J_{s,n}\tau_n = qn_pL_nS$. The quantities G_{d0} and C_{d0} appearing in Eqs. (44) and (45) as functions of V_0 are equal to

$$G_{d0}(V_0) = \frac{J_s \exp(\beta V_0)}{\kappa T/q} = \frac{qS}{\kappa T} \left(\frac{qp_n D_p}{L_p} + \frac{qn_p D_n}{L_n} \right) e^{qV_0/\kappa T}, \quad (46)$$

$$C_{d0}(V_0) = \frac{Q \exp(\beta V_0)}{2\kappa T/q} = \frac{qS}{\kappa T} \left(\frac{qp_n L_p}{2} + \frac{qn_p L_n}{2} \right) e^{qV_0/\kappa T}. \quad (47)$$

Expressions (46) and (47) correspond to the diffusion conductance and capacitance at low frequencies (when $\omega\tau_{p,n} \ll 1$ and $a_{p1}(\omega) = a_{n1}(\omega) \simeq 1$) for small signals (when $V_\sim \ll \kappa T/q$ and $g_1(V_\sim) \simeq 1$). Our expressions for G_{d0} and C_{d0} fully coincide with those given in a book [5] by Sze (see there formulas (65) and (66) of Chapter 2).

As seen from (44) and (45), the frequency dependence of the dynamic conductance $G_d(\omega)$ and the diffusion capacitance $C_d(\omega)$ is determined by the functions $a_{p1}(\omega)$ and $a_{n1}(\omega)$ given by formulas (10) and (12) with $k = 1$, whereas their dependence on the signal amplitude V_\sim is described by the function $g_1(V_\sim)$ introduced in the form of expression (43).

A certain simplification of expressions (44) and (45) occurs in the case of the *one-sided* $p^+ - n$ -junction with highly doped emitter when $p_n \gg n_p$, $J_{s,p} \gg J_{s,n}$, $Q_p \gg Q_n$ so that $J_s \simeq J_{s,p}$ and $Q \simeq Q_p$. Then

$$\frac{G_d(\omega, V_\sim)}{G_{d0}(V_0)} = \frac{\sqrt{1 + \sqrt{1 + \omega^2 \tau_p^2}}}{\sqrt{2}} \frac{I_1(\beta V_\sim)}{\beta V_\sim/2}, \quad (48)$$

$$\frac{C_d(\omega, V_\sim)}{C_{d0}(V_0)} = \frac{\sqrt{2}}{\sqrt{1 + \sqrt{1 + \omega^2 \tau_p^2}}} \frac{I_1(\beta V_\sim)}{\beta V_\sim/2}, \quad (49)$$

where from Eqs. (46) and (47) it follows that

$$G_{d0}(V_0) = \frac{2}{\tau_p} C_{d0}(V_0) = \frac{J_s \exp(\beta V_0)}{\kappa T/q}. \quad (50)$$

Frequency dependencies given by expressions (48) and (49) are plotted in Fig. 2. The plots differ from the similar curves shown by Sze [5] (see there Fig. 23 of Chapter 2) in that they take into account the signal amplitude influence owing to the factor $g_1(V_\sim) = I_1(\beta V_\sim)/(\beta V_\sim/2)$. For small signals (when $\beta V_\sim \ll 1$ and $g_1(V_\sim) \simeq 1$) our expressions (48) and (49) assume the form obtained by Sze [5] and are depicted by curves 1 in Fig. 2. The low-frequency values (when $\omega\tau_p \ll 1$) of the quantities (48) and (49) for arbitrary signals are equal to

$$\frac{G_d(0, V_\sim)}{G_{d0}(V_0)} = \frac{C_d(0, V_\sim)}{C_{d0}(V_0)} = \frac{I_1(\beta V_\sim)}{\beta V_\sim/2} \equiv g_1(V_\sim).$$

From here it follows that the low-frequency value (denoted by zero in parentheses that means $\omega = 0$) of the dynamic conductance is described by the following expression:

$$G_d(0, V_\sim) = G_{d0}(V_0) g_1(V_\sim). \quad (51)$$

Eq. (51) coincides with formula (A5) obtained from the conventional approach based on using the customary current-voltage characteristic for time-varying conditions.

The conventional approach is not able to provide the frequency dependence not only for $G_d(\omega)$ but also for $C_d(\omega)$ such as given by Eq. (48) and (49) which are valid for signals of arbitrary amplitude. The similar frequency dependency known from the published literature was obtained only for small signals when $V_\sim \ll \kappa T/q$. Such a result can be found, for example, in Sec. 2.4.4 of a book by Sze [5], where the curves $G_d(\omega)/G_{d0}$ and $C_d(\omega)/C_{d0}$ given in Fig. 23 correspond to our curves 1 in Fig. 2 calculated for $V_\sim = 0$. Other our curves denoted by numbers 2, 3, 4, 5 in Fig. 2 are novel since they demonstrate a dependence of the dynamic conductance and capacitance on the AC signal amplitude V_\sim , which was previously missed. It is this dependence that is of interest to check experimentally.

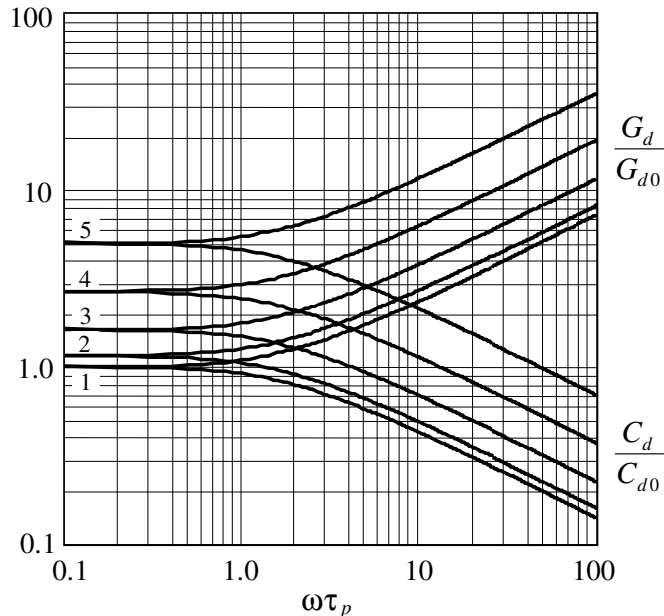


FIG. 2: Frequency dependencies of the normalized dynamic conductance $G_d(\omega)/G_{d0}$ and diffusion capacitance $C_d(\omega)/C_{d0}$ for different values of the signal voltage amplitudes: $V_{\sim} = 0$ (curve 1), $\kappa T/q$ (curve 2), $2\kappa T/q$ (curve 3), $3\kappa T/q$ (curve 4), $4\kappa T/q$ (curve 5).

VI. EXPERIMENTAL VALIDATION

The above theoretical results have been derived from the ideal Shockley's model which have a few simplifying assumptions. Among them the most essential ones are: (i) the large thickness of the neutral regions as compared with the minority-carrier diffusion lengths, i. e., $d_n \gg L_p$ and $d_p \gg L_n$; (ii) the neglect of recombination effects in the depletion layers owing to inequalities $W_n \ll L_p$ and $W_p \ll L_n$. Yet, such assumptions are rarely verified in practical conditions and should be taken into account, as applied to real devices used in our experiments.

The practically used p^+-n -diode with the one-sided injection has the thin n -base of thickness d_n compared to L_p . In this case, it is necessary to apply the boundary condition taking into account surface recombination on a metallic contact of the base located at $z = W_n + d_n$ (see Eq. (108) of Chapter 1 in Ref. [5]):

$$\left. \frac{\partial \Delta p(z, t)}{\partial z} \right|_{z=W_n+d_n} = -\frac{s_p}{D_p} \Delta p(W_n + d_n, t),$$

where s_p is the speed of surface recombination of holes (for ohmic contacts $s_p \rightarrow \infty$). The additional boundary condition changes only the saturation current by the factor A_p :

$$J_s = \frac{qp_n D_p}{L_p} S A_p \quad \text{with} \quad A_p = \frac{(s_p L_p / D_p) + \tanh((W_n + d_n) / L_p)}{1 + (s_p L_p / D_p) \tanh((W_n + d_n) / L_p)}. \quad (52)$$

As follows from Eq. (50), the measurement of the small-signal low-frequency conductance $G_{d0} = \beta J_s \exp(\beta V_0)$ will give us the saturation current (52) with allowance for the *surface recombination* on metallic contact of the base.

To take into account the *bulk recombination* processes in the depletion layer, let us follow a phenomenological approach suggested by Sze [5] and introduce the empirical nonideality factor n so as to provide the following replacement:

$$\beta \equiv \frac{q}{\kappa T} \rightarrow \frac{q}{n\kappa T} \equiv \beta_n. \quad (53)$$

Values of the factor n lie between 1 and 2 [5]: (a) $n = 1$ when contribution of the bulk recombination processes is negligibly small, (b) $n = 2$ when the recombination current dominates over the diffusion one.

By using the replacement (53), expression (51) for the low-frequency dynamic conductance can be rewritten in the following corrected form:

$$G_d(0, V_{\sim}) = G_{d0}(V_0) g_n(V_{\sim}), \quad (54)$$

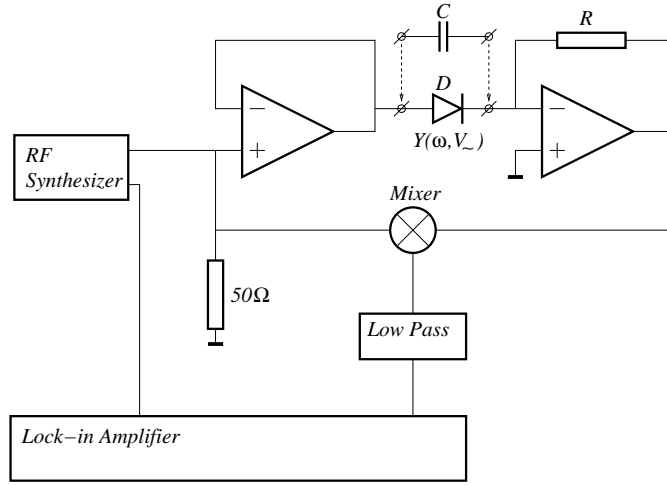


FIG. 3: Experimental setup with the measured diode D and reference capacitor C .

where the correcting function $g_n(V_{\sim})$ is defined as

$$g_n(V_{\sim}) = \frac{I_1(\beta_n V_{\sim})}{\beta_n V_{\sim}/2} \equiv \frac{I_1(\beta V_{\sim}/n)}{\beta V_{\sim}/2n}. \quad (55)$$

In general, the modified quantity β_n in expression (55) takes into account not only a contribution from the bulk recombination processes by means of the nonideality factor n but also that from a priori unknown temperature T of the $p-n$ -junction under experimental investigation. Hence, the product nT can be used as a fitting parameter to adjust the theoretical relations (54)–(55) with experimental results obtained below.

To verify our theory, we built a simple apparatus using the dual-phase DSP lock-in amplifier, Stanford Research Systems model SR830. For the low frequency measurement, the low noise electrometer grade operational amplifier, Burr-Brown OPA 128JM, is used. For the high-frequency measurements, the same lock-in amplifier, combined with a mixer, and high-frequency op-amps can be used, see Fig. 3. The AC voltage is applied to the diode with no bias ($V_0 = 0$). The lock-in amplifier has two displays — X and Y, which give the root-mean-square (rms) value of output signal at the excitation frequency ω . It is easy to show that the lock-in output in the X and Y displays is equal to

$$V_{out}^X = -RV_{in} \left[G_d(\omega) \cos(\phi - \phi_0) + \omega C_d(\omega) \sin(\phi - \phi_0) \right], \quad (56)$$

$$V_{out}^Y = -RV_{in} \left[G_d(\omega) \sin(\phi - \phi_0) + \omega C_d(\omega) \cos(\phi - \phi_0) \right]. \quad (57)$$

Here R is a feedback resistor, V_{in} is the rms value of the lock-in oscillator voltage ($V_{in} = V_{\sim}/\sqrt{2}$), ϕ is an internal phase of the lock-in oscillator signal connected to the phase detector, and ϕ_0 is a phase of the signal after passing through an external circuit. From (56) and (57) it follows that the two displays are $\pi/2$ out of phase from each other.

To get correct experimental values, it is necessary to adjust the phase ϕ of the lock-in local oscillator so that the X-display would be used for the conductance voltage $|V_{out}^X| = RV_{in}G_d$ and the Y-display for the capacitance voltage $|V_{out}^Y| = RV_{in}\omega C_d$. As follows from expressions (56) and (57), it can be realized only if $\phi = \phi_0$. The phase ϕ is adjusted with the reference capacitor C which is placed between the local oscillator and the minus input of the operational amplifier instead of diode D , as shown in Fig. 3. The phase adjustment is carried out until zero voltage is observed in the conductance X-display, i. e., when $\phi = \phi_0$. Then Eqs. (56) and (57) yield the required results:

$$G_d(\omega, V_{\sim}) = \frac{1}{R} \frac{|V_{out}^X|}{V_{in}} \Big|_{\phi=\phi_0}, \quad \omega C_d(\omega, V_{\sim}) = \frac{1}{R} \frac{|V_{out}^Y|}{V_{in}} \Big|_{\phi=\phi_0}. \quad (58)$$

After the adjustment, the reference capacitor C is replaced by the measured diode D and the measurements are performed by varying the applied AC voltage V_{\sim} with $V_0 = 0$. The operating frequency of the lock-in internal oscillator was chosen 1 kHz to surely provide the relation $\omega\tau_p \ll 1$ underlying the initial theoretical expression (51). To extract the conductance, one must normalize the data.

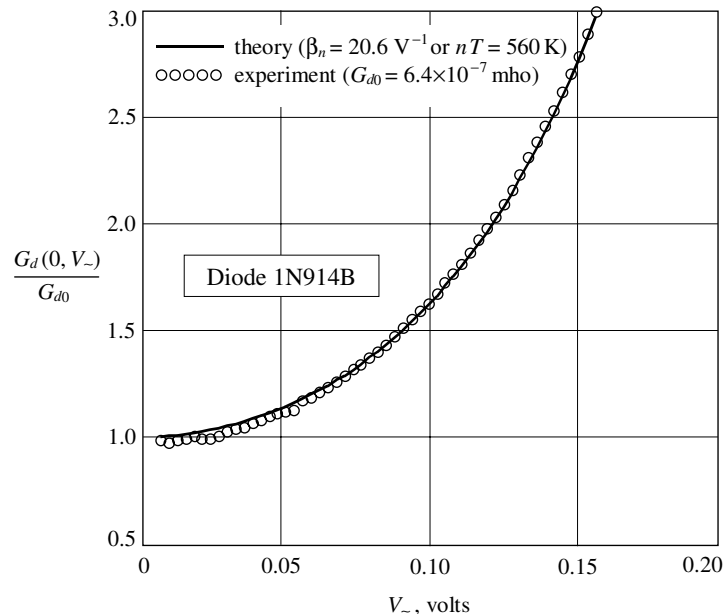


FIG. 4: Theoretical and experimental dependencies of the normalized dynamic conductance $G_d(0, V_{\sim})/G_{d0}$ on the peak voltage V_{\sim} of AC signal for the 1N914B diode with no DC bias ($V_0 = 0$).

For our experiments, we have employed a common high frequency diode 1N914B. The experimental results for the above-mentioned diode are presented in Fig. 4 which demonstrates a quite satisfactory agreement between the experimental data and our theoretical results, in the low frequency range. All resistors and capacitors employed in the experiment were measured with the Stanford Research Systems model SR720 LCR meter. The measurement error is found to be below 1%. In an additional paper, the detailed experimental results will be presented.

As seen from Eqs. (54) and (55), the small voltage measurement (when $g_n = 1$) gives a value of the low-frequency dynamic conductance G_{d0} defined by formula (50). This value has proved to be equal $G_{d0} \simeq 6.4 \times 10^{-7}$ mho. From here it follows that $J_s = G_{d0}/\beta_n = 31$ nA, which is in agreement with the reverse current for the 1N914B diode given by manufacturers.

From the experimental curve plotted in Fig. 4 it follows that the modified factor $\beta_n \equiv q/n\kappa T$ should be equal to 20.6 for the 1N914B diode in order to fit the theoretical expression (54). Hence, the fitting parameter nT is equal to 560 K, which for the operating temperature $T = 400$ K provides the nonideality factor $n = 1.4$. Therefore, the measured diode operates in a regime when the diffusion current slightly dominates over the recombination current.

VII. CONCLUSION

Spectral approach to the theory of $p-n$ -junctions has allowed us to take into account the effect of large signal at both the low and high frequencies as compared to $\tau_{p,n}^{-1}$. This approach is based on the known diffusion equations for injected minority carriers, which is a standard practice for semiconductor electronics.

The only specific feature distinguishing our approach from the conventional one given for comparison in Appendix is related to the initial representation of the desired carrier concentrations in the form of Fourier expansion over frequency harmonics. Such harmonics are produced by nonlinear processes in the $p-n$ -junction when the sufficiently large AC voltage $V_1 = V_{\sim}/2$ is applied to the junction together with the DC bias voltage V_0 . As a result, the spectra of both the excess concentration of injected carriers and the external circuit current have been derived (see formulas (25), (26), and (32)). The use of appropriate terms in Fourier series has given rise to expressions for the DC component J_0 and AC component J_1 of the external circuit current. The former determine the static current–voltage characteristic $J_0(V_0)$ (formula (34)) and from the latter follows the dynamic admittance $Y(\omega) = J_1/V_1$ (formulas (37)–(39)). These expressions have proved to be dependent not only on V_0 but also on V_1 , in the case of the nonlinear (in signal) regime of operation of the $p-n$ -junction.

The results are corroborated by experimental verification, as follows from Fig. 4. Detailed experimental results will be presented in a separated paper.

APPENDIX A: CONVENTIONAL APPROACH TO ANALYSIS OF THE CURRENT–VOLTAGE CHARACTERISTIC FOR p – n -DIODES

Conventional theory of the p – n -diode operation under the AC signal of arbitrary amplitude is based on generalizing the known expression for the static current–voltage characteristic to time-varying conditions:

$$J(t) = J_s(e^{\beta v(t)} - 1). \quad (\text{A1})$$

Here the total voltage $v(t)$ applied to the diode includes the DC bias voltage V_0 and the harmonic signal voltage $V_\sim \cos \omega t$ (see Eq. (5)). After substituting (5) into Eq. (A1), it is necessary to use the following Fourier series [6] (see also formula 8.511.4 in [7]):

$$e^{\beta V_\sim \cos \omega t} = I_0(\beta V_\sim) + 2I_1(\beta V_\sim) \cos \omega t + 2I_2(\beta V_\sim) \cos 2\omega t + \dots, \quad (\text{A2})$$

where I_0, I_1, I_2, \dots are the modified Bessel functions of first kind. Insertion of the Fourier series (A2) into expression (A1) yields

$$J(t) = J_s \left\{ \left[I_0(\beta V_\sim) e^{\beta V_0} - 1 \right] + 2I_1(\beta V_\sim) e^{\beta V_0} \cos \omega t + 2I_2(\beta V_\sim) e^{\beta V_0} \cos 2\omega t + \dots \right\}. \quad (\text{A3})$$

Expression (A3) is the Fourier expansion of the diode current whose DC component gives the static current–voltage characteristic

$$J_0(V_0, V_\sim) = J_s \left[I_0(\beta V_\sim) e^{\beta V_0} - 1 \right], \quad (\text{A4})$$

which is valid for the harmonic signal of arbitrary amplitude V_\sim . The first harmonic of the current (A3) allows one to obtain the dynamic conductance

$$G_d(V_0, V_\sim) = \frac{J_s \exp(\beta V_0)}{\kappa T/q} \frac{I_1(\beta V_\sim)}{\beta V_\sim/2} \equiv G_{d0}(V_0) g_1(V_\sim), \quad (\text{A5})$$

where $G_{d0}(V_0)$ and $g_1(V_\sim)$ are given by formulas (46) and (43).

Expression (A5) resulting from the conventional approach describes solely the low-frequency dynamic conductance G_d (cf. Eq. (51)), whose frequency dependence can be obtained only by using the spectral approach, as it is done in Sec. V. Moreover, our spectral approach yields not only $G_d(\omega)$ but also $C_d(\omega)$ for arbitrary signals. In the case of small signals, the similar frequency dependencies are derived in the literature (for example, see [5]), but they never follow from the current–voltage characteristic in the form of Eq. (A1) taken as an initial point for derivation.

ACKNOWLEDGEMENTS

We thank CNPq/“Instituto do Milênio” Initiative. One of the authors, AAB, also thanks CNPq for the support during his stay at UFPE.

REFERENCES

-
- [1] W. Shockley, “The theory of p – n -junctions in semiconductors and p – n -junction transistors,” *Bell Syst. Tech. J.*, vol. 28, pp. 435–454, 1949.
 - [2] C. T. Sah, R. N. Noyce, and W. Shockley, “Carrier generation and recombination in p – n -junctions and p – n -junction characteristics,” *Proc. IRE*, vol. 45, pp. 1228–1243, 1957.
 - [3] J. L. Moll, “The evolution of the theory of the current – voltage characteristics of p – n -junctions,” *Proc. IRE*, vol. 46, pp. 1076–1085, 1958.

- [4] R. A. Smith, *Semiconductors*, 2nd ed., London: Cambridge University Press, 1979.
- [5] S. M. Sze, *Physics of Semiconductor Devices*, 2nd ed., New York: Wiley, 1981.
- [6] B. Schiek, *Meßsysteme der Hochfrequenztechnik*, Heidelberg: Hüthig, 1984.
- [7] I. S. Gradshteyn and I. M. Ryzhik, *Tables of Integrals, Series, and Products*. New York: Academic Press, 1980.
- [8] The authors are grateful to a referee for indicating this reference.